Proc. Natl. Acad. Sci. USA
Vol. 95, pp. 12169–12173, October 1998
Biochemistry

Enhanced transcription factor access to arrays of histone H3/H4 tetramer·DNA complexes *in vitro*: Implications for replication and transcription

(chromatin/TFIIIA/nucleosome/DNA flexibility/analytical ultracentrifugation)

CHRISTIN TSE*, TERACE M. FLETCHER*, AND JEFFREY C. HANSEN†

Department of Biochemistry, University of Texas Health Science Center, 7703 Floyd Curl Drive, San Antonio, TX 78284-7760

Communicated by Jack Gorski, University of Wisconsin, Madison, WI, August 24, 1998 (received for review May 5, 1998)

ABSTRACT **Defined model systems consisting of physiologically spaced arrays of H3/H4 tetramer·5S rDNA complexes have been assembled *in vitro* from pure components. Analytical hydrodynamic and electrophoretic studies have revealed that the structural features of H3/H4 tetramer arrays closely resemble those of naked DNA. The reptation in agarose gels of H3/H4 tetramer arrays is essentially indistinguishable from naked DNA, the gel-free mobility of H3/H4 tetramer arrays relative to naked DNA is reduced by only 6% compared with 20% for nucleosomal arrays, and H3/H4 tetramer arrays are incapable of folding under ionic conditions where nucleosomal arrays are extensively folded. We further show that the cognate binding sites for transcription factor TFIIIA are significantly more accessible when the rDNA is complexed with H3/H4 tetramers than with histone octamers. These results suggest that the processes of DNA replication and transcription have evolved to exploit the unique structural properties of H3/H4 tetramer arrays.**

The mechanism of replication-coupled chromatin assembly has been characterized extensively *in vivo*. Immediately after DNA synthesis, short stretches of parental nucleosomes are deposited in a dispersive manner on each DNA strand (reviewed in refs. 1–3). *De novo* nucleosome assembly subsequently occurs on the regions of naked DNA sandwiched between the parental nucleosomal arrays. The mechanism of *de novo* nucleosome assembly is sequential, involving initial deposition of histones H3/H4, followed by addition of histones H2A/H2B to form nucleosomal arrays, and finally incorporation of linker histones to form mature chromatin (4–7). The core histones are believed to be deposited as H3/H4 tetramers and H2A/H2B dimers (1–3). Importantly, dispersive segregation of parental nucleosomes and subsequent H3/H4 tetramer deposition occur within as little as 1–2 min after replication and together comprise the initial nucleoprotein assembly that can be detected *in vivo* (5, 6). Once this intermediate is formed, H2A/H2B dimers bind rapidly while incorporation of linker histones takes ≈10–15 min (7–9). Deposition of histones *in vivo* appears to be mediated by a complex of chromatin assembly factors (10).

Because of the staged nature of replication-coupled nucleosome assembly, there potentially is a window of time in which other nucleoprotein assemblies can be incorporated onto specific regions of newly replicated DNA, depending on how they interact with H3/H4 tetramer arrays. In this regard, competition between transcription factor binding and nucleosome assembly at the time of replication has been documented both *in vivo* (11, 12) and *in vitro* (13) and has been hypothesized to be a general mechanism for establishing either active or repressive states of promoters and genes (11, 14, 15). In addition, an enhanced ability of regulatory proteins to interact with H3/H4 tetramer arrays compared with nucleosomal arrays also may be relevant to transcription and chromatin remodeling (reviewed in refs. 1, 3, and 16).

Structural-based investigations of these questions to date have focused on individual H3/H4 tetramer–DNA complexes (17). To better mimic the nucleoprotein configurations present *in vivo* after replication and likely during transcription, in this work we have assembled physiologically spaced arrays of H3/H4 tetramer–DNA complexes *in vitro* from purified H3/H4 tetramers and tandemly repeated 5S rDNA. Results indicate that the conformational and electrostatic properties of H3/H4 tetramer arrays much more closely resemble naked DNA than nucleosomal arrays under physiological ionic conditions. We further demonstrate that increased accessibility of the transcription factor TFIIIA to H3/H4 tetramer arrays compared with nucleosomal arrays arises directly from the intrinsic differences in the physicochemical properties of these two types of nucleohistone complexes.

EXPERIMENTAL PROCEDURES

Materials. The 208-12 DNA template, which consists of 12 tandem 208-bp repeats of a fragment of the *Lytechinus* 5S rRNA gene (18), and bacteriophage T3 were isolated as described (19, 20). Histone octamers and H3/H4 tetramers were purified by stepwise elution from hydroxylapatite columns as described (19, 21). TFIIIA was provided by J. J. Hayes (University of Rochester) after purification by the method of Smith *et al.* (22). Molecular biology grade LE agarose was obtained from Research Organics.

Salt Dialysis Reconstitution. Nucleosomal and H3/H4 tetramer arrays were reconstituted by salt dialysis from 208-12 DNA and either chicken erythrocyte core histone octamers or H3/H4 tetramers, respectively, as described (23). The mol histones/mol 208-bp DNA (r) ranged from 0.2 to 1.2. The DNA concentration was 100 μg/ml. The final dialysis step was against 10 mM Tris·HCl and 0.25 mM EDTA (pH 7.8) (TE) buffer. Reconstitutes subsequently were analyzed by sedimentation velocity in TE buffer, and the average number of histone octamers or H3/H4 tetramers bound per 208-12 DNA (N) was determined from plots of the log of the average sedimentation coefficient (s^{avg}) versus r as described (24).

Agarose Gel Electrophoresis. Electrophoretic parameters of nucleosomal arrays, H3/H4 tetramer arrays, naked 208-12 DNA, and bacteriophage T3 were determined in 0.2–3.0% agarose multigels as described (24, 25). Briefly, multigels were cast in 40 mM Tris·HCl and 1.0 mM EDTA (pH 7.8) running

The publication costs of this article were defrayed in part by page charge payment. This article must therefore be hereby marked "*advertisement*" in accordance with 18 U.S.C. §1734 solely to indicate this fact.

*C.T. and T.M.F. contributed equally to this work.
†To whom reprint request should be addressed. e-mail: hansen@bioc02.uthscsa.edu.

buffer containing either 0 (E buffer) or 2.0 mM free $MgCl_2$ (EM buffer). Samples were dialyzed against the same running buffer for 4 h at 4°C before electrophoresis. Multigels were electrophoresed for 7–8 h at 1 V/cm. Running buffer was circulated throughout the experiment at a temperature of 24 ± 3°C. Sample mobilities (μ) in each running gel were measured from the ethidium bromide-stained multigel using NIH IMAGE imaging software. The gel-free μ (μ'_o) was obtained by extrapolating the linear region of a semilogarithmic plot of log μ vs. agarose concentration using a standard least-squares linear regression ($r^2 = 0.99–1.0$). The (μ'_o subsequently was corrected for electro-osmosis and normalized to yield the μ_o as described (24, 25). For each different running gel, the experimentally determined μ, (μ'_o and the known radius (R_e) of bacteriophage T3 (30.1 nm), were used to calculate the average gel pore radius (P_e) using the formula, $\mu/(\mu'_o = (1 - R_e/P_e)^2$ (26, 27). The R_e of nucleosomal arrays and DNA in each gel subsequently was determined from their experimentally determined μ and (μ'_o and the calculated P_e by using the same formula (24, 25).

Analytical Ultracentrifugation. Sedimentation velocity studies were performed in a Beckman XL-A analytical ultracentrifuge equipped with scanner optics as described (25, 28). Scans were analyzed by the method of van Holde and Weischet (29) to yield the integral distribution of sedimentation coefficients using Ultrascan data analysis software (B. Demeler, University of Texas Health Science Center, San Antonio, TX). The s^{avg} was obtained from the $s_{20,w}$ value at boundary fraction = 0.5 of the distribution plot (23, 24).

TFIIIA Binding Assays. TFIIIA was incubated for 45 min at room temperature with either naked 208-12 DNA, H3/H4 tetramer arrays, or nucleosomal arrays. Binding reactions contained 40 mM Tris·HCl, 90 mM KCl, 2 mM $MgCl_2$, 10 μM $ZnCl_2$, and 2.5 mM DTT (pH 7.5). The mixtures subsequently either were electrophoresed on 0.8% agarose gels buffered with 20 mM Tris-borate (pH 7.5) or were digested with 15 units of *Eco*RI for 90 min at room temperature and the digestion products electrophoresed on native 5% polyacrylamide gels buffered with 40 mM Tris-borate (pH 7.5).

RESULTS

Conformational and Electrostatic Properties of H3/H4 Tetramer Arrays. The H3/H4 tetramer and histone octamer adopt identical translational positions on 5S rDNA (17, 30). However, when reconstituted onto a 200-bp fragment, significantly less DNA is wrapped around an H3/H4 tetramer than an intact histone octamer (17). Thus, we first determined the amount of DNA bound to each H3/H4 tetramer when components of an array. To accomplish this, we utilized the 208-12 DNA template, which contains twelve 208-bp repeats of the *Lytechinus* 5S rRNA gene. Various numbers of H3/H4 tetramers or histone octamers were assembled onto this DNA, and the reconstitutes were analyzed by sedimentation velocity to determine the s^{avg} and from it the frictional coefficient (f), and by quantitative agarose gel electrophoresis to determine the effective radius in dilute gels (R_e^{dil}). Both the f and R_e^{dil} yield a precise measurement of the shape and length of the array (24, 31), which in turn provides a sensitive indication of the amount of DNA bound to each histone–DNA complex (32, 33). Fig. 1 shows the results of experiments performed in low salt buffer, where the arrays are maximally extended (19, 28). For both nucleosomal arrays and H3/H4 tetramer arrays, the f and R_e decreased identically with increasing histone occupancy of the 5S repeats. At array saturation (i.e., $n = 12$), the f and R_e^{dil} of H3/H4 tetramer arrays both were ≈35% greater than the corresponding values determined for nucleosomal arrays, indicating that H3/H4 tetramer arrays are substantially more elongated in low salt buffer than nucleosomal arrays. Importantly, the 35% larger f and R_e^{dil} demonstrate that only ≈120–125 bp‡ of DNA was organized by each H3/H4 tetramer of the array, consistent with that observed for single H3/H4 tetramer–DNA complexes (17). In addition, these results also rigorously establish that the f measured in the analytical ultracentrifuge and the R_e measured in dilute agarose gels provide identical information regarding the shape of chromatin molecules in solution.

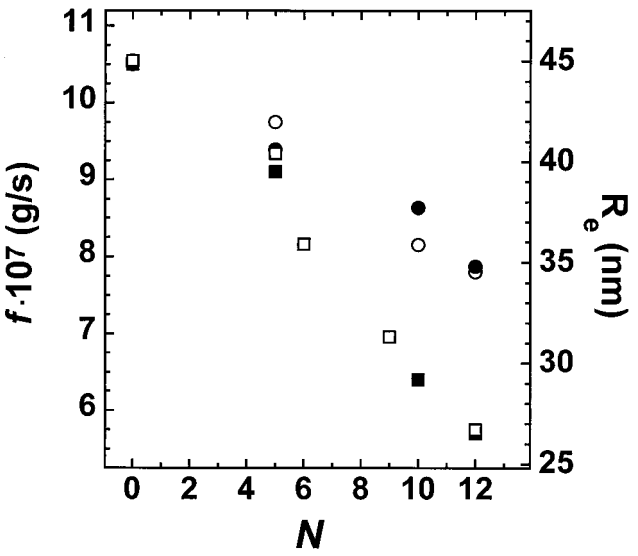

FIG. 1. Changes in the f and R_e^{dil} of H3/H4 tetramer arrays and nucleosomal arrays as a function of 208-12 DNA saturation. Sedimentation velocity experiments were performed in TE buffer and quantitative agarose gel electrophoresis experiments in E buffer. The f was calculated from the $s_{20,w}$ in TE by using standard procedures (41). The f and R_e^{dil} of H3/H4 tetramer arrays are indicated by the closed circles and open circles, respectively, whereas the f and R_e^{dil} of nucleosomal arrays are indicated by closed and open squares, respectively.

A structural parameter that can strongly influence macromolecular interactions is surface charge. To determine the surface charge properties of H3/H4 tetramer arrays, quantitative agarose gel electrophoresis was used to measure the gel-free mobility (μ_o) in low salt buffer. The μ_o is directly proportional to the average surface charge density of macromolecules (34) and is obtained by extrapolating the linear region of a plot of log mobility versus agarose percentage to 0% agarose (24, 25). The μ_o in low salt buffer of H3/H4 tetramer arrays decreased linearly with increasing array saturation (Fig. 2), as observed previously for nucleosomal arrays (24). At array saturation, the μ_o of an H3/H4 tetramer array was only 6% lower than that of naked DNA. This compares to a 20% decrease for nucleosomal arrays (Fig. 2, *Inset*). Thus, the bulk of the decrease in DNA surface charge density associated with nucleosome assembly results from interaction of H2A/H2B dimers with the H3/H4 tetramer·DNA complex.

We next determined the influence of salt on the properties of the reconstitutes. The 12-mer nucleosomal arrays fold extensively in buffers containing divalent cations, causing the s^{avg} to increase from 29S in low salt to 40S in 2 mM $MgCl_2$ (28, 31). Previous sedimentation analyses showed that the folding of nucleosomal arrays in $MgCl_2$/KCl mixtures was markedly reduced in the absence of H2A/H2B dimers, with only a small salt-dependent increase in the s^{avg} of these tetramer arrays

‡The experimentally determined $s_{20,w}$ for a 12-mer tetramer array in low salt (19S) was modeled by using Kirkwood Theory. By using a value of 9S for a single H3/H4 central particle (15) and assuming the array is extended, an average linker DNA length of ≈85 bp must be present to yield a 19S sedimentation coefficient. Consequently, for the 208-12 system, only ≈120–125 bp of DNA must be bound to each H3/H4 tetramer.

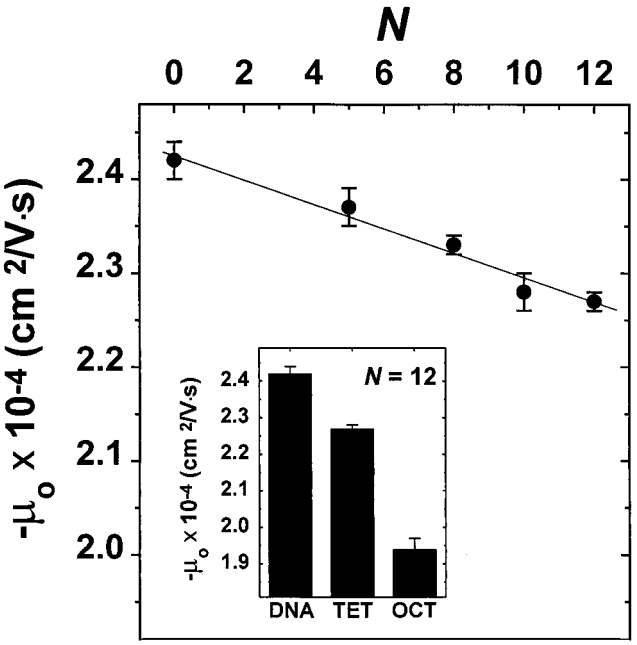

FIG. 2. Changes in the m_o of H3/H4 tetramer arrays in E buffer as a function of 208-12 DNA saturation. Data points represent the mean ± 1 SD of three to four determinations. The *Inset* shows the μ_o of naked 208-12 DNA (DNA) (24), trypsinized nucleosomal arrays (TRP) (33), H3/H4 tetramer arrays (TET), and nucleosomal arrays (OCT) (24).

(35). This change in s^{avg} was proposed to reflect a small residual ability of H3/H4 tetramer arrays to fold in high salt (35). To more carefully examine the molecular basis of salt effects on the structure of H3/H4 tetramer arrays, we measured the s^{avg}, R_e^{dil}, and μ_o in 2 mM $MgCl_2$. Results indicated that the s^{avg} of H3/H4 tetramer arrays increased by ≈10% (Table 1), consistent with previous results (35). Furthermore, the R_e^{dil} decreased by 10%. By comparison, the s^{avg} of nucleosomal arrays increased by ≈40% (28, 31) and R_e^{dil} decreased by ≈30% (31) under identical ionic conditions. Measurement of the μ_o of these complexes yielded complementary results. In 2 mM $MgCl_2$ the μ_o of naked 208-12 DNA decreases by 25% relative to 60% for folded 40S nucleosomal arrays (31). This result compares to a 35% decrease in the μ_o of H3/H4 tetramer arrays in 2 mM $MgCl_2$ (data not shown). Cumulatively, the hydrodynamic and electrophoretic results confirm that H3/H4 tetramer arrays undergo a small conformational change in the presence of Mg^{2+}.

Analysis of the conformational flexibility of H3/H4 tetramer arrays allowed us to delineate the molecular basis of this structural change. A measure of array flexibility was obtained by using quantitative agarose gel electrophoresis to determine the R_e in 0.9–3.0% gels. With increasing gel concentration, the P_e gradually decreases and eventually approaches the R_e of the macromolecule being electrophoresed. At this point, flexible macromolecules deform during electrophoresis in a process called reptation. Reptation manifests as a decreasing R_e with decreasing P_e (24, 25, 27). This finding is in contrast to the behavior inflexible, nonreptating macromolecules, where the R_e remains constant at all P_e (24–26). The R_e of naked 208-12 DNA in low salt buffer decreased from 35 to 27 nm as the P_e decreased from 140 to 40 nm, with the sharpest decrease occurring below P_e = 60 nm (Fig. 3). In contrast, the R_e of saturated nucleosomal arrays remained constant at 26–27 nm over the same P_e range. Both of these results are essentially identical to those obtained previously under the same experimental conditions (24). In the case of H3/H4 tetramer arrays, the R_e in low salt buffer decreased dramatically at $P_e \leq 140$ nm, and the R_e values at any given P_e were only slightly reduced compared with the R_e of naked 208-12 DNA (Fig. 3). Furthermore, when examined in 2 mM $MgCl_2$, the R_e of H3/H4 tetramer arrays at $P_e \leq 140$ nm were indistinguishable from the corresponding values measured in E (Fig. 3). This is in distinct contrast to nucleosomal arrays in 2 mM $MgCl_2$, which are folded and have a constant R_e of 21 nm (Fig. 3; ref. 31). Cumulatively, our electrophoretic and hydrodynamic analyses in low and high salt have yielded several important observations. First, they demonstrate that H3/H4 tetramer arrays remain essentially as flexible as naked DNA despite the fact that ≥120 bp of DNA are organized by each tetramer. In addition, the data in Fig. 3 very clearly show that H3/H4 tetramer arrays are unable to fold in 2 mM $MgCl_2$. Consequently, the small conformational change that occurs in Mg^{2+} most likely reflects a small increase in the amount of DNA wrapped around each H3/H4 tetramer in the presence of salt, analogous to what occurs with trypsinized nucleosomal arrays in NaCl (32) and $MgCl_2$ (33, 36).

Interaction of TFIIIA with H3/H4 Tetramer Arrays and Nucleosomal Arrays. As described above, there are marked differences in intrinsic physicochemical properties of H3/H4 tetramer arrays compared with nucleosomal arrays. These results suggest that cognate sites for DNA binding proteins may be more accessible when DNA is organized into H3/H4 tetramer arrays, which behave more like naked DNA, as

Table 1. Effect of salt on the s^{avg} and R_e^{dil} of H3/H4 tetramer and nucleosomal arrays

	H3/H4 tetramer arrays		Nucleosomal arrays	
Buffer	s^{avg}, S	R_e^{dil}, nm	s^{avg}, S	R_e^{dil}, nm
E	19	35 ± 0.3	29	27.0 ± 0.2
EM	21	32 ± 0.9	40	21.0 ± 0.3

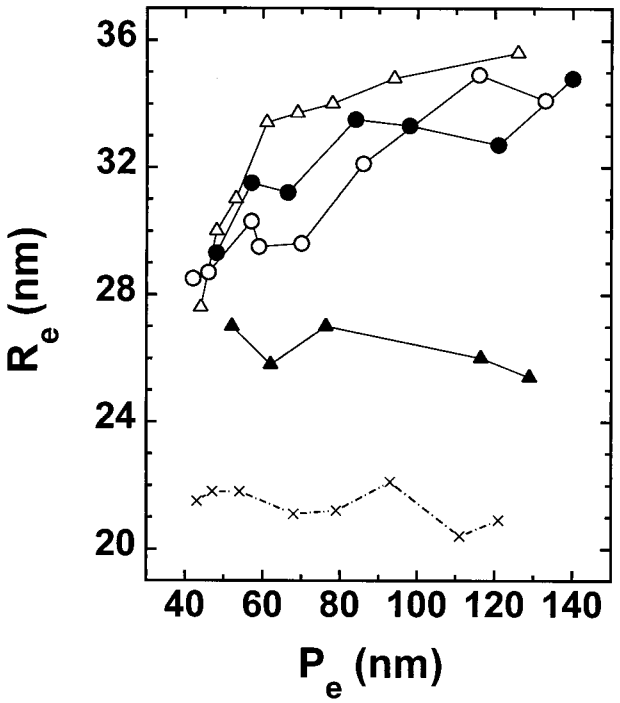

FIG. 3. P_e-dependence of the R_e of naked 208-12 DNA in E buffer (△), H3/H4 tetramer arrays in E (○), and EM buffer (●), and nucleosomal arrays in E (△) and EM (×) buffer. The R_e values were determined in multigels whose agarose percentage ranged from 0.9 to 3.0%. The data are representative of the results obtained in two to six separate experiments for each DNA and reconstitute sample. The data for nucleosomal arrays in EM buffer were taken from ref. 31.

opposed to nucleosomal arrays and bulk chromatin. To test this idea, we compared the binding of transcription factor TFIIIA to 208-12 reconstitutes assembled from H3/H4 tetramers or intact histone octamers. Each 208-bp 5S repeat of the 208-12 DNA contains a specific TFIIIA binding site located near the 3′ edge of the major nucleosome positioning frame (37). To assay for TFIIIA binding, reconstitutes were incubated with TFIIIA and digested with *Eco*RI, which cuts at the junction of each 5S repeat (18, 36). The relative amounts of naked 5S rDNA repeats and nucleoprotein complexes subsequently were determined using native PAGE. Addition of increasing amounts of TFIIIA to naked 208-12 DNA led to formation of increasing amounts of a slower migrating TFIIIA-5S rDNA band after *Eco*RI digestion (data not shown; see Fig. 4 *A* and *B*). Binding of *Xenopus* TFIIIA to *Lytechinus* 5S rDNA is consistent with the fact that 208-12 DNA can be transcribed efficiently by RNA polymerase III in *Xenopus* oocyte nuclear extracts (35, 38). We next determined the ability of TFIIIA to bind to H3/H4 tetramer arrays. Subsaturated templates containing an average of six bound H3/H4 tetramers per 208-12 DNA ($n = 6$) were used in these experiments to allow TFIIIA binding to occur under conditions where there was equal amounts of naked 5S repeats and H3/H4·5S rDNA complexes within the array population. In addition, $n = 6$ nucleosomal arrays are incapable of folding (31), thereby allowing a direct comparison of TFIIIA binding to DNA organized by H3/H4 tetramers and histone octamers. Results indicated that TFIIIA bound nearly equally well to naked DNA repeats and H3/H4–DNA complexes; formation of TFIIIA·H3/H4 tetramer·5S DNA ternary complexes could be detected at TFIIIA concentrations only slightly higher than needed for TFIIIA to bind to naked 5S rDNA, and occurred before TFIIIA had bound to all available naked 5S rDNA binding sites (Fig. 4*A*). Thus, the affinity of TFIIIA for its 5S rDNA binding sites was only slightly reduced after assembly of H3/H4 tetramers onto the rDNA repeats.

Equivalent experiments subsequently were performed with $n = 6$ nucleosomal arrays. At TFIIIA concentrations that yielded significant amounts of both TFIIIA·5S rDNA complexes and TFIIIA·H3/H4 tetramer·5S rDNA ternary complexes, no TFIIIA binding to 5S rDNA complexed with histone octamers could be detected (Fig. 4*B*). A faintly detectable band presumably corresponding to a TFIIIA·nucleosome complex was detected after incubations of nucleosomal arrays with very high TFIIIA concentrations (data not shown). This result could reflect either some residual affinity of TFIIIA for the nucleosome or binding of TFIIIA to naked DNA sites present on the small fraction of rDNA repeats that contains an alternatively positioned histone octamer. Nevertheless, the data in Fig. 4*B* establish clearly that the accessibility of TFIIIA to rDNA complexed with only H3/H4 tetramers was enhanced significantly compared with rDNA assembled into nucleosomal arrays. Importantly, to ensure that the TFIIIA binding observed in Fig. 4 *A* and *B* did not occur after restriction digestion, naked 208-12 DNA and $n = 12$ H3/H4 tetramer arrays were incubated with TFIIIA and the mixtures electrophoresed on a 0.8% agarose gel. In both cases, addition of TFIIIA led to a marked reduction in mobility of the entire sample (Fig. 4*C*). These results demonstrate stoichiometric interaction of TFIIIA with 208-12 DNA and H3/H4 tetramer arrays before *Eco*RI digestion.

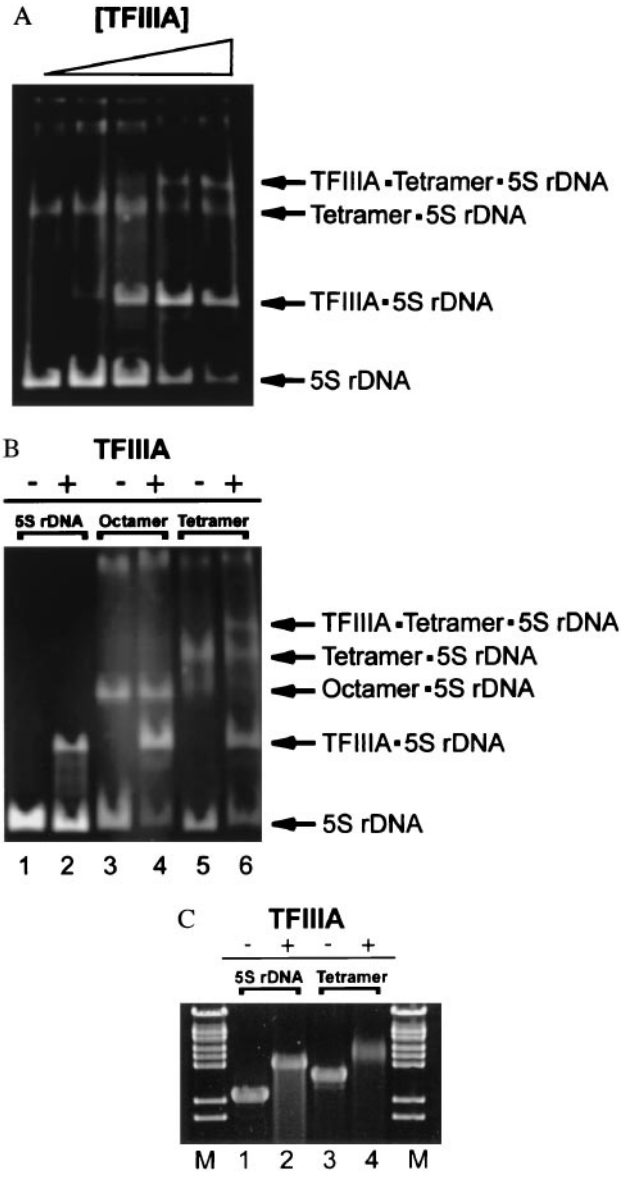

FIG. 4. Binding of TFIIIA to 208-12 DNA complexed with H3/H4 tetramers or histone octamers. (*A*) Binding of TFIIIA to partially saturated tetramer·DNA complexes. Increasing amounts of TFIIIA (0.5–3.75 μg) was incubated with 1.5 μg of $n = 6$ 208-12 tetramer arrays and digested with *Eco*RI, which cuts at the junction of each 5S repeat (see *Experimental Procedures*). The digestion products subsequently were resolved on a 5% native polyacrylamide gel at 15 mA, constant current. (*B*) Comparison of the binding of TFIIIA to nucleosomal arrays and H3/H4 tetramer arrays. Naked 208-12 DNA, $n = 6$ 208-12 nucleosomal arrays, and $n = 6$ H3/H4 tetramer arrays (1.5 μg each) were incubated with 3.75 μg of TFIIIA and digested with *Eco*RI. Samples were electrophoresed on a 5% native polyacrylamide gel as in *A*. Lanes 1, 3, and 5 correspond to naked DNA, nucleosomal arrays, and H3/H4 tetramer arrays incubated in the absence of TFIIIA, respectively. Lanes 2, 4, and 6 correspond to the same samples incubated with TFIIIA. (*C*) Agarose gel electrophoresis of TFIIIA·DNA and TFIIIA·H3/H4 tetramer array complexes before *Eco*RI digestion. Naked 208-12 DNA (DNA) and $n = 12$ H3/H4 tetramer arrays (Tetramer) were incubated with saturating levels of TFIIIA as described, followed by electrophoresis for 3 h at 60 V (constant volts) on a 0.8% agarose gel buffered with 20 mM Tris-borate (pH 7.5). Lanes 1 and 3 correspond to naked DNA and $n = 12$ 208-12 tetramer arrays incubated in the absence of TFIIIA, respectively. Lanes 2 and 4 correspond to naked DNA and $n = 12$ 208-12 tetramer arrays incubated with TFIIIA, respectively. λ DNA–*Bst*EII digest was used as a marker (M).

DISCUSSION

Our studies have demonstrated that the surface charge density and conformational flexibility of physiologically spaced H3/H4 tetramer arrays are remarkably similar to those of naked DNA and fundamentally different than the corresponding properties of nucleosomal arrays (Figs. 2 and 3). Furthermore, whereas nucleosomal arrays are extensively folded under physiological ionic conditions, H3/H4 tetramer arrays remain unfolded (Fig. 3; ref. 35). Finally, H3/H4 tetramer

arrays allow much greater access of TFIIIA to its cognate binding sites than occurs with nucleosomal arrays, even when the latter is unfolded (Fig. 4). All of these results presumably arise at least in part from the fact that each H3/H4 tetramer of the array organizes substantially less DNA than does a histone octamer (Fig. 1).

Elucidation of the structural features of H3/H4 tetramer arrays have made it possible to rigorously describe the global higher order organization of a key functional nucleoprotein intermediate present immediately after DNA replication *in vivo*. This intermediate is formed when short stretches of ≈3–7 parental nucleosomes are dispersively deposited onto the two DNA strands, followed by rapid factor-mediated deposition of H3/H4 tetramers on the intervening DNA (reviewed in refs. 1–3). The parental nucleosomes retain their original levels of histone H1 and HMG proteins, and their core histones remain underacetylated (5, 8, 39, 40). Hence, the stretches of parental chromatin will be at least partially condensed under physiological ionic conditions and may even form a 30-nm conformation if the array is long enough. Together with the decreased DNA accessibility resulting from the nucleosomes *per se* (Fig. 4; ref. 17), the regions of parental chromatin will be strongly refractory to transcription factor binding. In distinct contrast, the intervening H3/H4 tetramer arrays will be completely unfolded, very DNA-like in terms of their flexibility and surface charge density, and significantly more accessible to transcription factors. In terms of factor binding, it remains to be determined whether all of the DNA organized by the H3/H4 tetramer is more accessible to transcription factors or only that DNA closer to the particle periphery. Nevertheless, these data establish that there is a direct physicochemical basis for competition between transcription factor binding and nucleosome assembly immediately after replication (11–15). Importantly, whether the stretches of H3/H4 tetramer arrays mature into bulk chromatin or become programmed into transcriptionally active genes largely will depend on both the local concentrations of H2A/H2B dimers and transcription factors in the vicinity of the replication fork and their respective affinities for H3/H4 tetramer·DNA complexes. In this regard, it seems likely that the mechanisms required to precisely regulate these parameters throughout the entire genome have evolved in conjunction with the unique nucleoprotein structure that is formed on each DNA strand immediately after replication *in vivo*.

1. Wolffe, A. P. (1995) *Chromatin: Structure and Function* (Academic, New York), 2nd Ed.
2. Sobel, R. E., Cook, R. G., Perry, C. A., Annunziato, A. T. & Allis, C. D. (1995) *Proc. Natl. Acad. Sci. USA* **92,** 1237–1241.
3. Fletcher, T. M. & Hansen, J. C. (1996) *Crit. Rev. Eukaryotic Gene Expression* **6,** 149–188.
4. Worcel, A., Han, S. & Wong, M. L. (1978) *Cell* **15,** 969–977.
5. Jackson, V. & Chalkley, R. (1981) *J. Biol. Chem.* **256,** 5095–5103.
6. Annunziato, A. T., Schindler, R. K., Riggs, M. G. & Seale, R. L. (1982) *J. Biol. Chem.* **257,** 8507–8515.
7. Smith, D. R., Jackson, I. J. & Brown, D. D. (1984) *Cell* **37,** 645–652.
8. Annunziato, A. T., Schindler, R. K., Thomas, C. A., Jr., & Seale, R. L. (1981) *J. Biol. Chem.* **256,** 11880–11886.
9. Gasser, R., Koller, T. & Sogo, J. M. (1996) *J. Mol. Biol.* **258,** 224–239.
10. Ito, T., Tyler, J. K. & Kadonaga, J. T. (1997) *Genes Cells* **2,** 593–600.
11. Almouzni, G. & Wolffe, A. P. (1993) *Exp. Cell Res.* **205,** 1–15.
12. Barton, C. M. & Emerson, B. M. (1994) *Genes Dev.* **8,** 2453–2465.
13. Almouzni, G., Mechali, M. & Wolffe, A. P. (1991) *Mol. Cell. Biol.* **11,** 655–665.
14. Wolffe, A. P. (1994) *Cell* **77,** 13–16.
15. Van Holde, K. E. (1985) *Physical Biochemistry* (Prentice-Hall, Englewood Cliffs, NJ), 2nd Ed.
16. Peterson, C. L. & Tamkun, J. W. (1995) *Trends Biochem. Sci* **20,** 143–146.
17. Hayes, J. J. & Wolffe, A. P. (1992) *Proc. Natl. Acad. Sci. USA* **89,** 1229–1233.
18. Simpson, R. T., Thoma, F. & Brubaker, J. M. (1985) *Cell* **42,** 799–808.
19. Hansen, J. C., Ausio, J., Stanik, V. H. & van Holde, K. E. (1989) *Biochemistry* **28,** 9129–9136.
20. Serwer, P., Watson, R. H., Hayes, S. L. & Allen, J. L. (1983) *J. Mol. Biol.* **170,** 447–469.
21. Simon, R. T. & Felsenfeld, G. (1979) *Nucleic Acids Res.* **6,** 689–696.
22. Smith D. R., Jackson, I. J. & Brown, D. D. (1984) *Cell* **37,** 645–652.
23. Hansen, J. C. & Lohr, D. (1993) *J. Biol. Chem.* **268,** 5840–5848.
24. Fletcher, T. M., Krishnan, U., Serwer, P. & Hansen, J. C. (1994) *Biochemistry* **33,** 2226–2233.
25. Hansen, J. C., Kreider, J. I., Demeler, B. & Fletcher, T. M. (1997) *Methods* **12,** 62–72.
26. Griess, G. A., Moreno, E. T., Easom, R. & Serwer, P. (1989) *Biopolymers* **28,** 1475–1484.
27. Griess, G. A., Moreno, E. T., Herrmann, R. & Serwer, P. (1990) *Biopolymers* **29,** 1277–1287.
28. Schwarz, P. M. & Hansen, J. C. (1994) *J. Biol. Chem.* **269,** 16284–16289.
29. van Holde, K. E. & Weischet, W. O. (1978) *Biopolymers* **17,** 1387–1403.
30. Dong, F. & van Holde, K. E. (1991) *Proc. Natl. Acad. Sci. USA* **88,** 10596–10600.
31. Fletcher, T. M., Serwer, P. & Hansen, J. C. (1994) *Biochemistry* **33,** 10859–10863.
32. Garcia-Ramirez, M., Dong, F. & Ausio, J. (1992) *J. Biol. Chem.* **267,** 19587–19595.
33. Fletcher, T. M. & Hansen, J. C. (1995) *J. Biol. Chem.* **270,** 25359–25362.
34. Shaw, O. (1978) *Electrophoresis* (Academic, London).
35. Hansen, J. C. & Wolffe, A. P. (1994) *Proc. Natl. Acad. Sci. USA* **91,** 2339–2343.
36. Tse, C. & Hansen, J. C. (1997) *Biochemistry* **36,** 11381–11388.
37. Simpson, R. T. and Stafford, D. W. (1983) *Proc. Natl. Acad. Sci. USA* **80,** 51–55.
38. Hansen, J. C. & Wolffe, A. P. (1992) *Biochemistry* **31,** 7977–7988.
39. Perry, C. A. & Annunziato, A. T. (1989) *Nucleic Acids Res.* **17,** 4275–4291.
40. Perry, C. A., Dadd, C. A., Allis, C. D. & Annunziato, A. T. (1993) *Biochemistry* **32,** 13605–13614.